Supporting Information

Synthesis of Ru(II) cyclometallated complexes via C(aryl)-S bond activation: X-ray structure, DNA/BSA protein binding and antiproliferative activity

Akash Das,[a] Subrata Mandal,[a] Rimi Mukherjee,[b] Rahul Naskar,[a] Nabendu Murmu[b] and Tapan K. Mondal*[a]

[a]Department of Chemistry, Jadavpur University, Kolkata- 700032, India. E-mail: tapank.mondal@jadavpuruniversity.in

[b]Department of Signal Transduction and Biogenic Amines (STBA), Chittaranjan National Cancer Institute, Kolkata- 700026, India.

CONTENTS

Fig. S1: ^{1}H-NMR spectrum of ligand HL^1-SEt in $CDCl_3$
Fig. S2: ^{1}H-NMR spectrum of ligand HL^2-SMe in $CDCl_3$
Fig. S3: ^{1}H-NMR spectrum of [Ru(L^1)(CO)(PPh$_3$)$_2$] (**1**) complex in $CDCl_3$
Fig. S4: ^{1}H-NMR spectrum of [Ru(L^2)(CO)(PPh$_3$)$_2$] (**2**) complex in $CDCl_3$
Fig. S5: ^{13}C-NMR spectrum of ligand HL^1-SEt in $CDCl_3$
Fig. S6: ^{13}C-NMR spectrum of ligand HL^2-SMe in $CDCl_3$
Fig. S7: HRMS of ligand HL^1-SEt
Fig. S8: HRMS of ligand HL^2-SMe
Fig. S9: HRMS of [Ru(L^1)(CO)(PPh$_3$)$_2$] (**1**) complex
Fig. S10: HRMS of [Ru(L^2)(CO)(PPh$_3$)$_2$] (**2**) complex
Fig. S11: IR spectrum of ligand HL^1-SEt
Fig. S12: IR spectrum of ligand HL^2-SMe
Fig. S13: IR spectrum of [Ru(L^1)(CO)(PPh$_3$)$_2$] (**1**) complex
Fig. S14: IR spectrum of [Ru(L^2)(CO)(PPh$_3$)$_2$] (**2**) complex
Table S1: Crystallographic data and refinement parameters of complexes **1** and **2**
Table S2: Selected X-ray and calculated bond distances and angles of complexes **1** and **2**
Table S3: Energy and composition of some selected molecular orbitals of complex **1**
Table S4: Energy and composition of some selected molecular orbitals of complex **2**
Table S5: Vertical electronic transition calculated by TDDFT/CPCM method of complexes **1** and **2**
Fig. S15: Contour plots of some selected molecular orbital of **1**
Fig. S16: Contour plots of some selected molecular orbital of **2**
Fig. S17: Plot of log [(F_o-F)/F] versus log [complex] of complexes **1** (A) and **2** (B)
Fig. S18: Percentage cell viability measured for HL^1-SEt (A) and HL^2-SMe (B) against MCF-7
Fig. S19: Percentage cell viability measured for complex **1** (A) and **2** (B) against MCF-7
Fig. S20: UV spectra of the metal complexes **1**(A) and **2**(B), showing their stability in 1:10 DMSO /buffer medium at 0 and 24 h.
Fig. S21: Absorption spectra of complexes (—) and after addition of BSA (—).

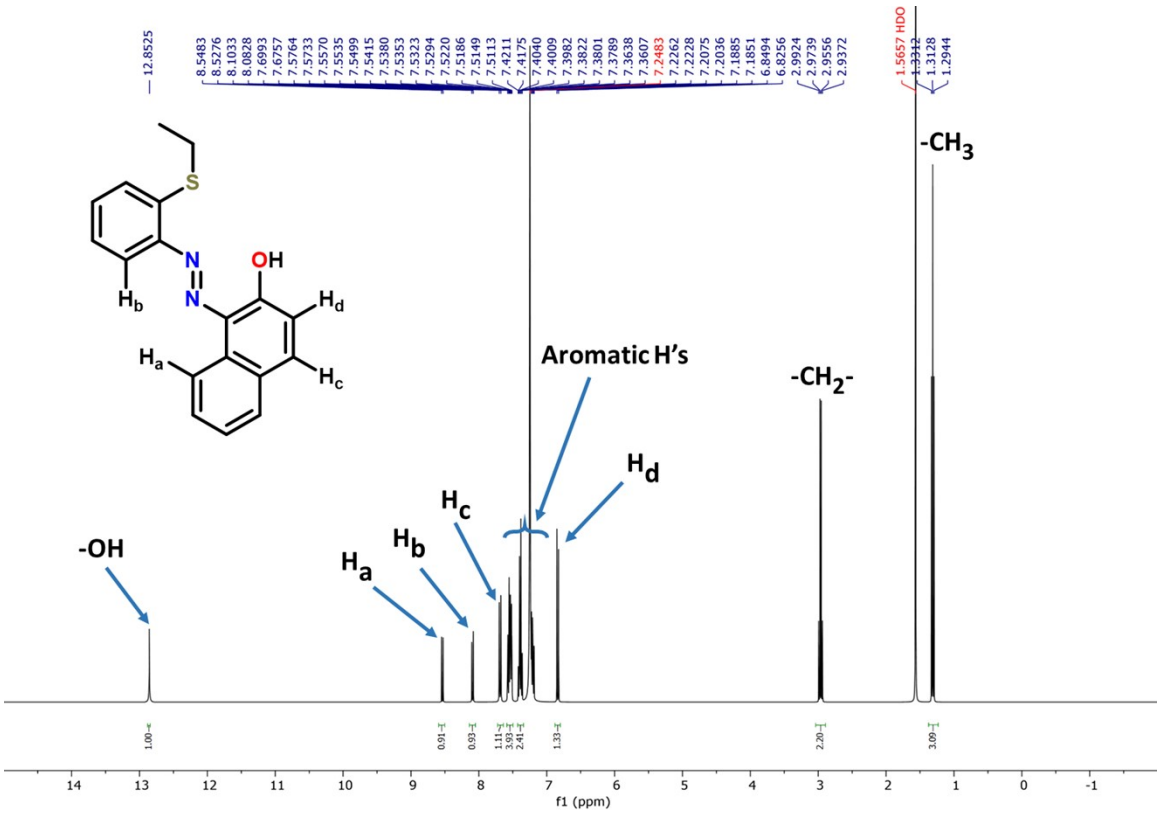

Figure S1: ^{1}H-NMR spectrum of ligand HL^{1}-SEt in $CDCl_3$

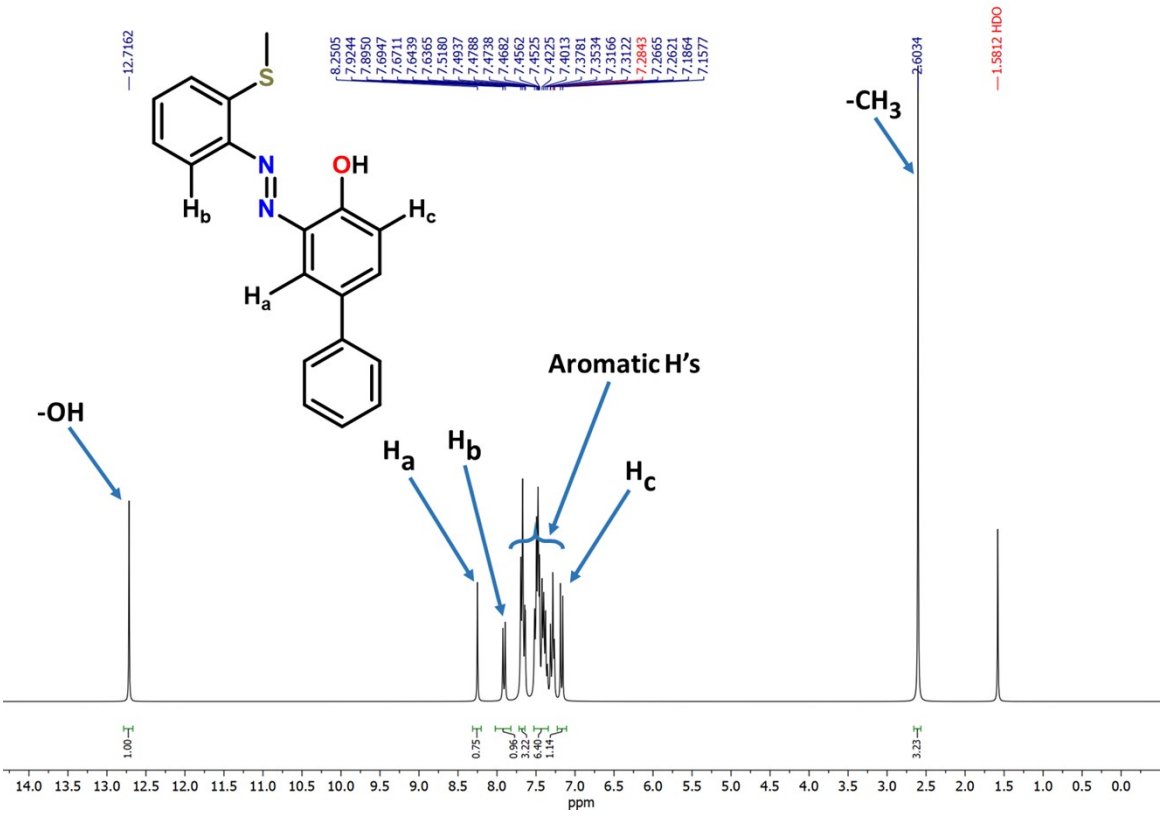

Figure S2: ^{1}H-NMR spectrum of ligand HL^{2}-SMe in $CDCl_3$

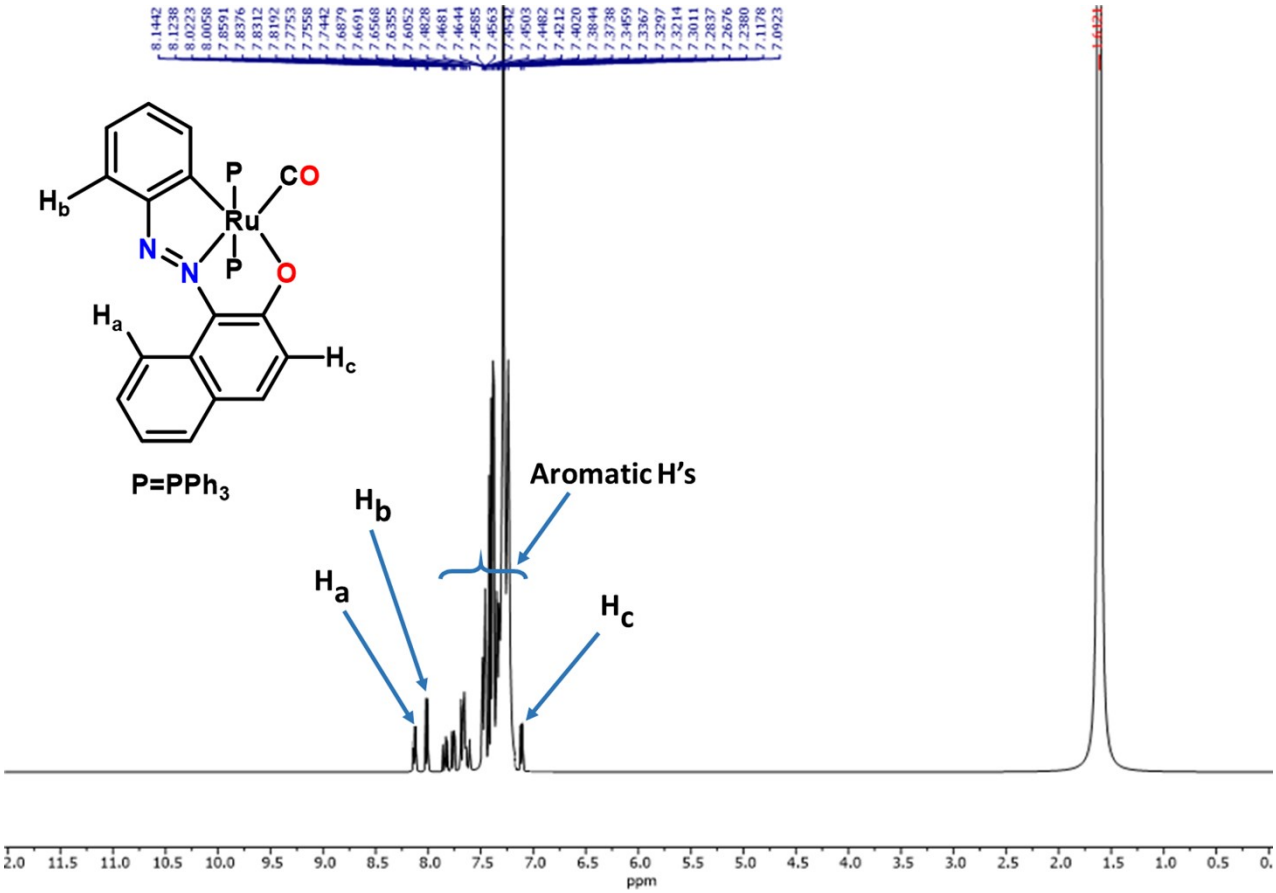

Figure S3: ^{1}H-NMR spectrum of [Ru(L^{1})(CO)(PPh_3)$_2$] (**1**) complex in $CDCl_3$

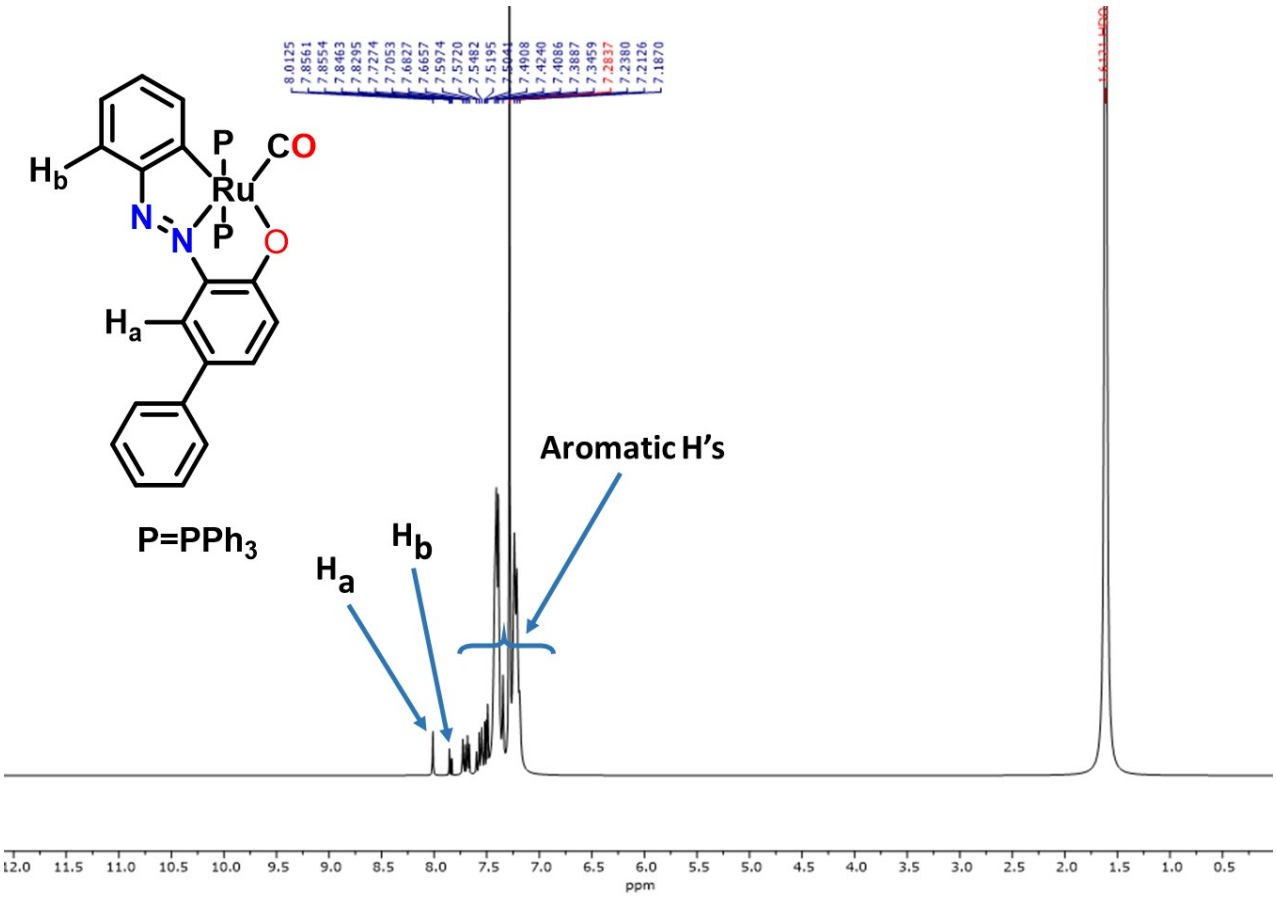

Figure S4: ^{1}H-NMR spectrum of [Ru(L^{2})(CO)(PPh_3)$_2$] (**2**) complex in $CDCl_3$

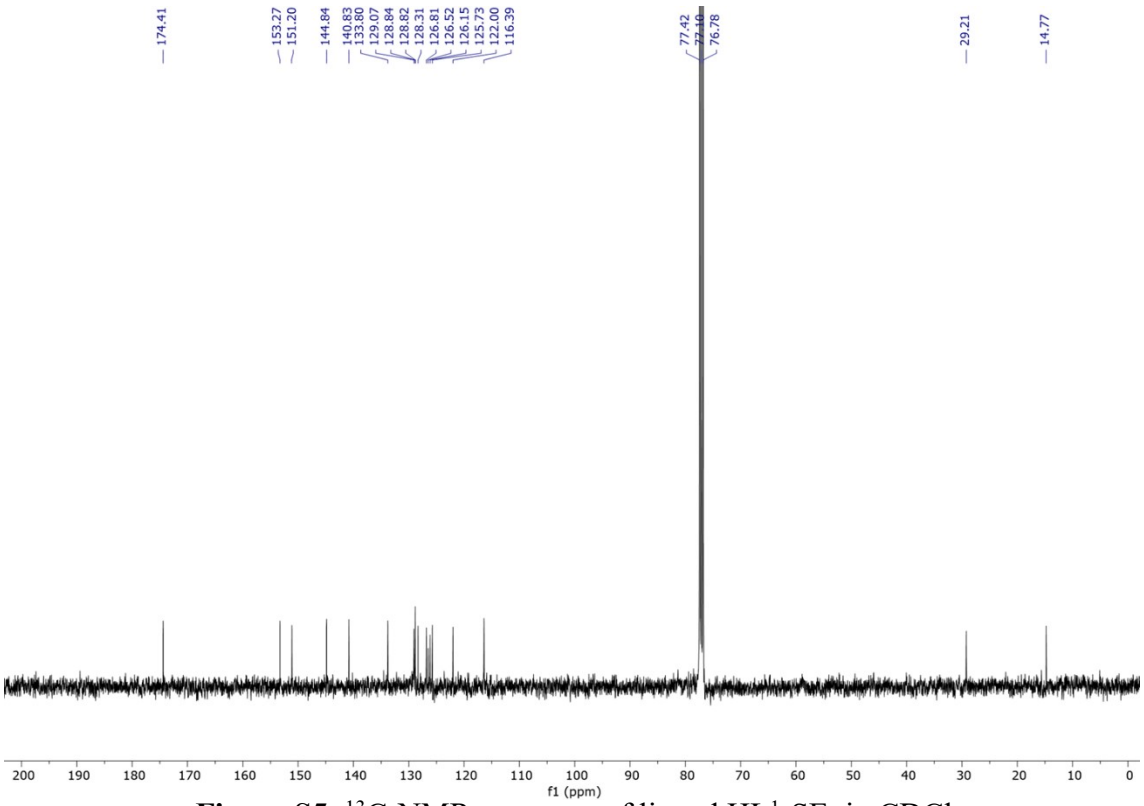

Figure S5: ^{13}C-NMR spectrum of ligand HL^{1}-SEt in $CDCl_3$

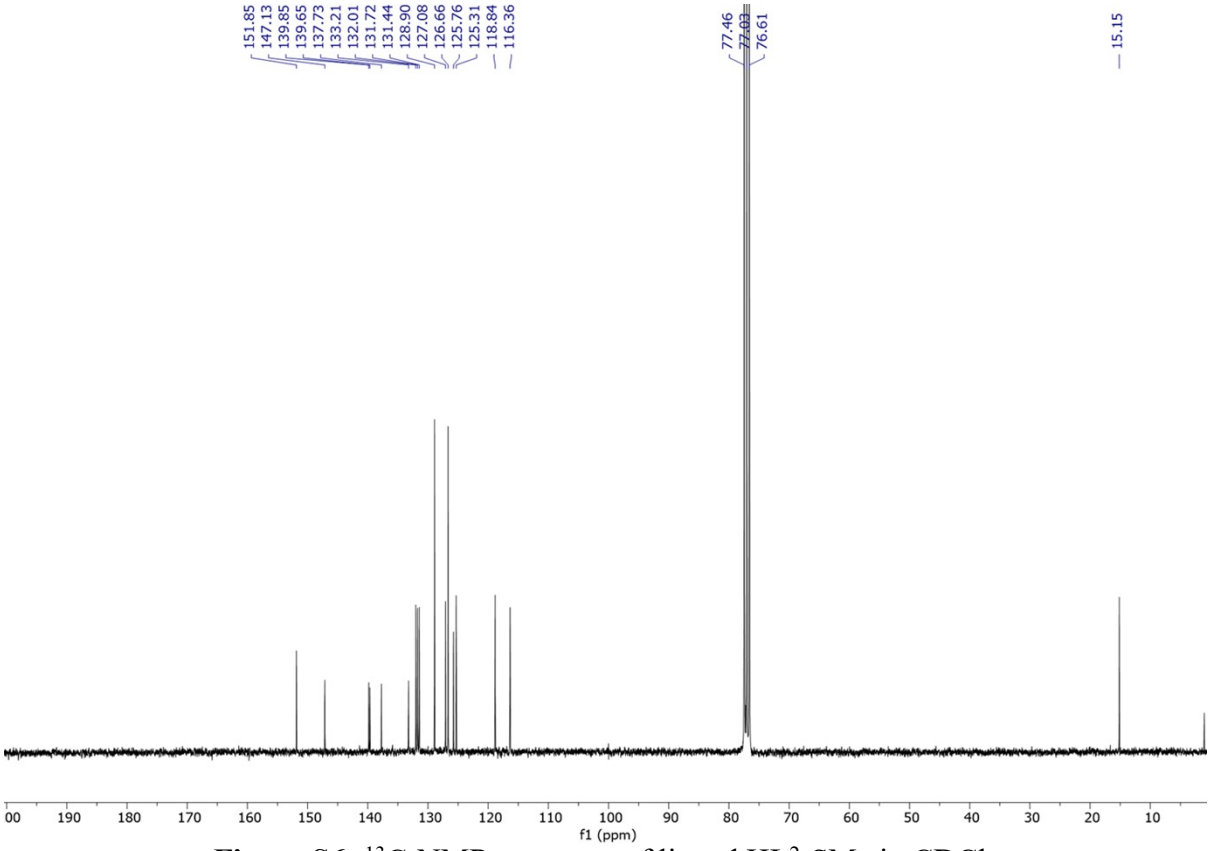

Figure S6: ^{13}C-NMR spectrum of ligand HL^{2}-SMe in $CDCl_3$

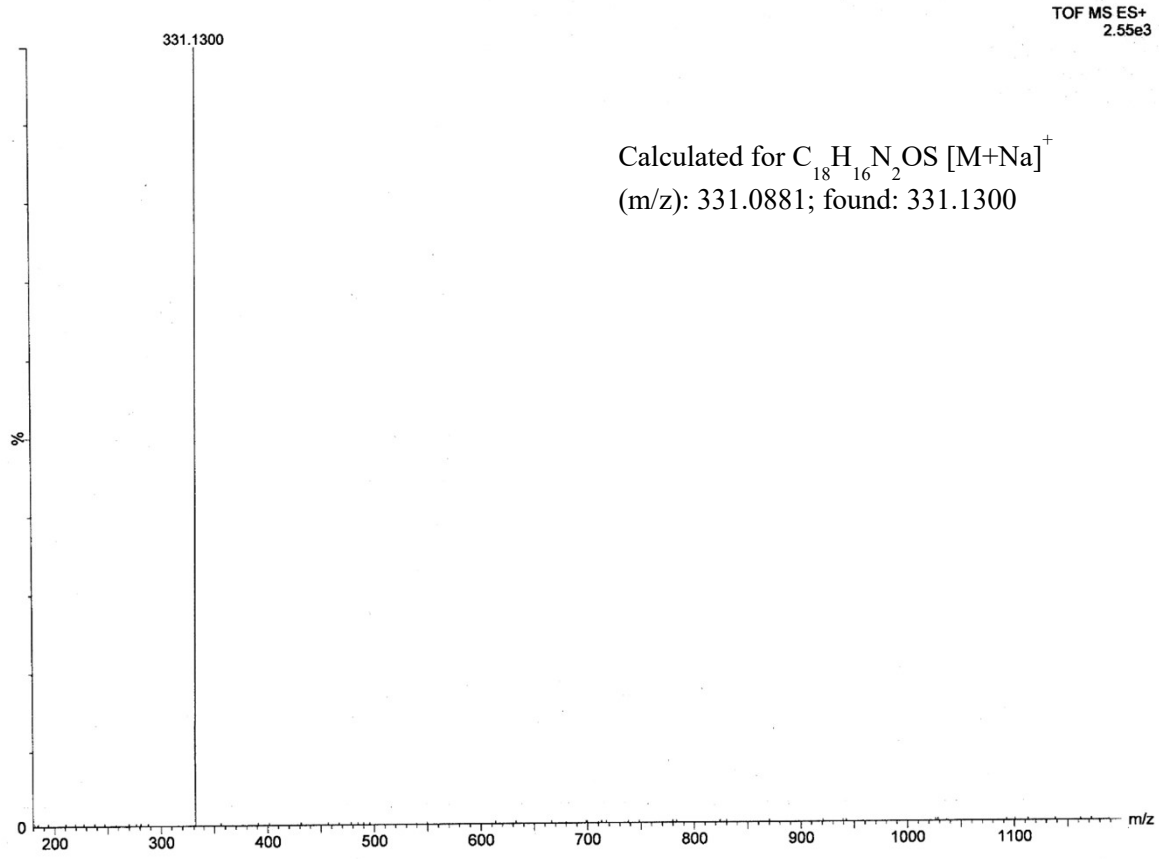

Calculated for $C_{18}H_{16}N_2OS\ [M+Na]^+$
(m/z): 331.0881; found: 331.1300

Figure S7: HRMS of ligand HL^1-SEt

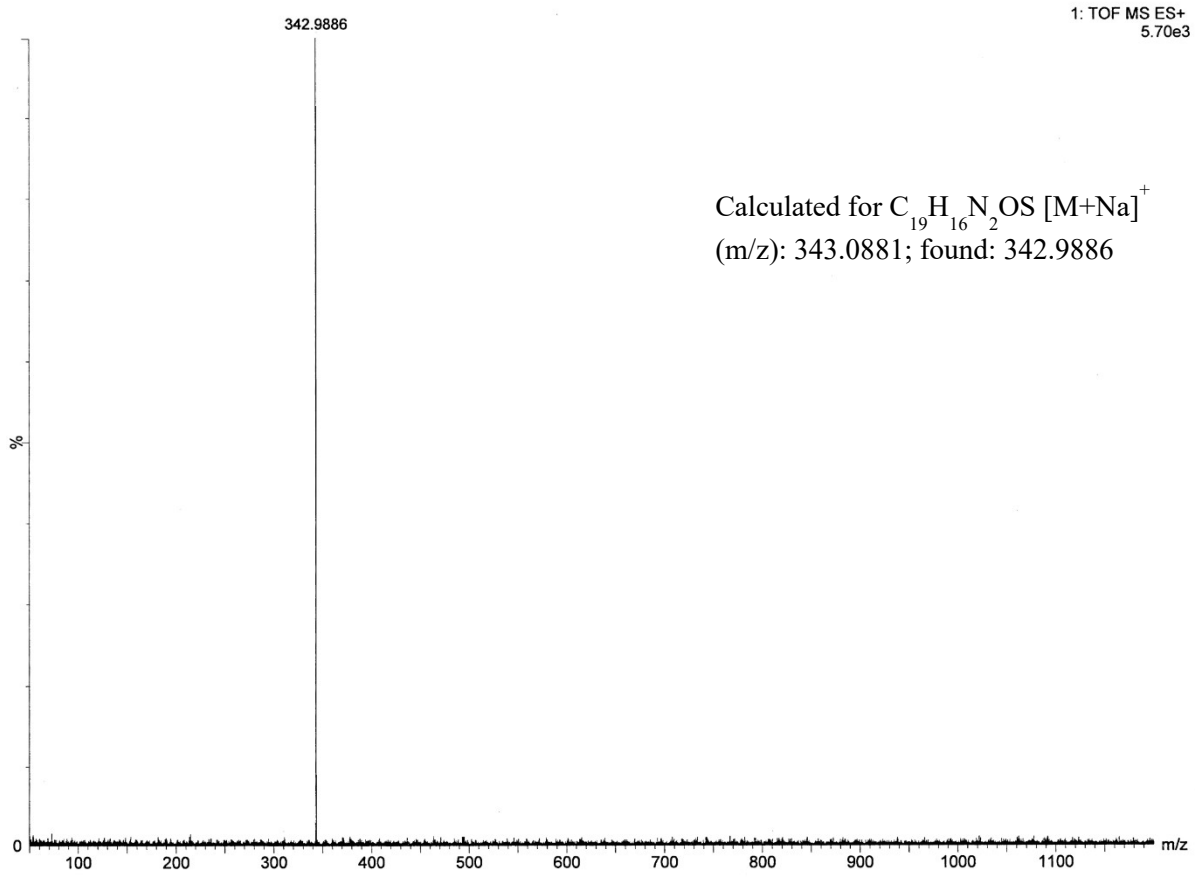

Calculated for $C_{19}H_{16}N_2OS\ [M+Na]^+$
(m/z): 343.0881; found: 342.9886

Figure S8: HRMS of ligand HL^2-SMe

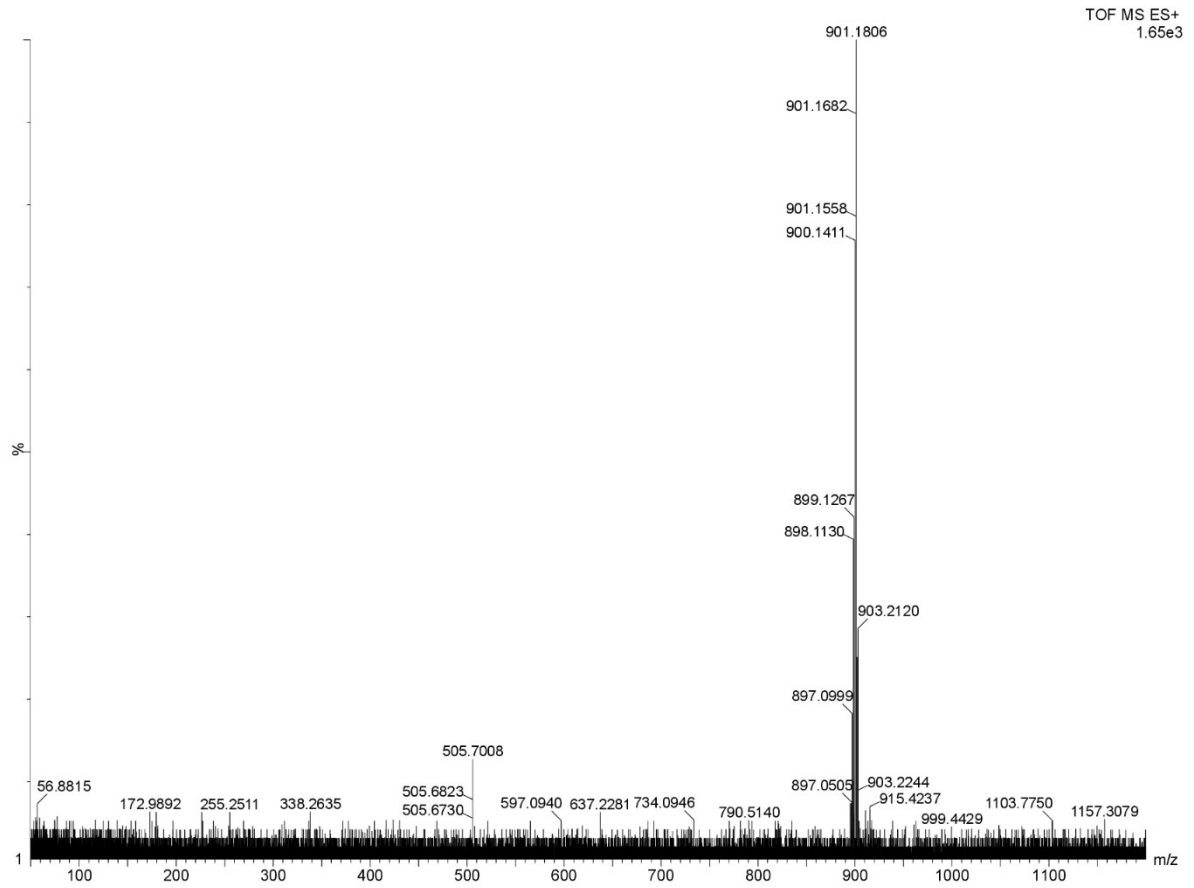

Figure S9: HRMS of $[Ru(L^1)(CO)(PPh_3)_2]$ (**1**) complex

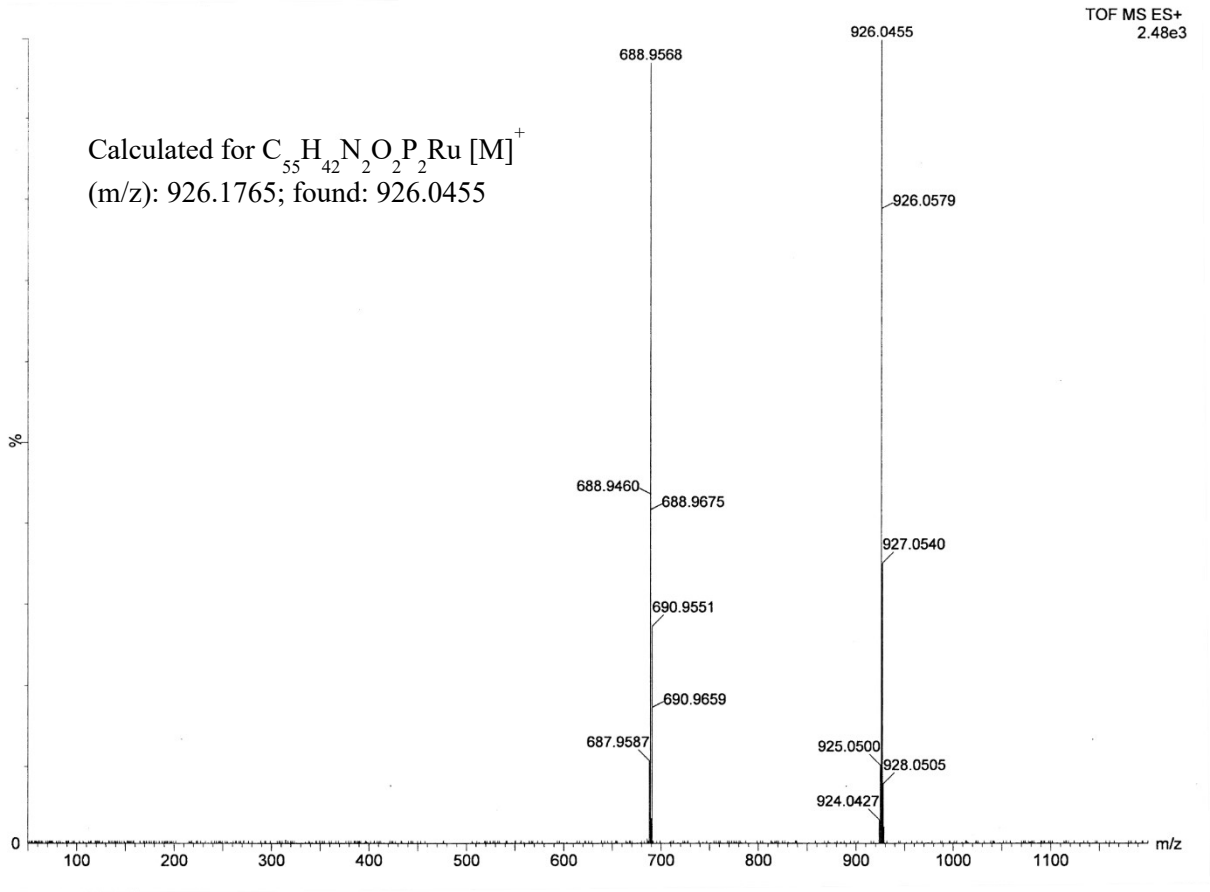

Figure S10: HRMS of $[Ru(L^2)(CO)(PPh_3)_2]$ (**2**) complex

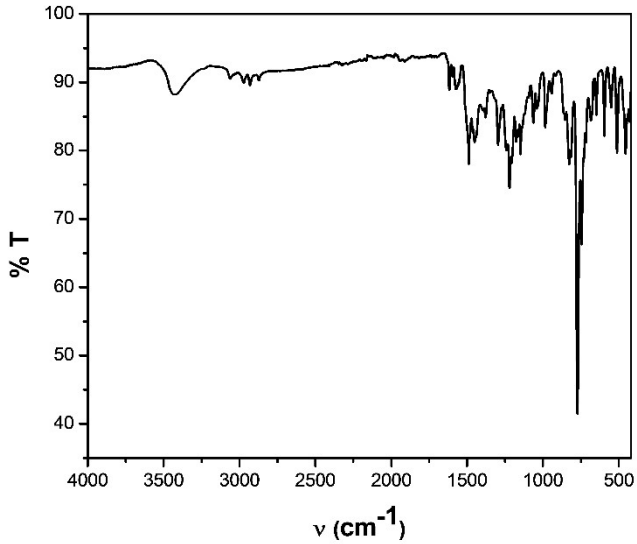

Figure S11: IR spectrum of ligand HL^1-SEt

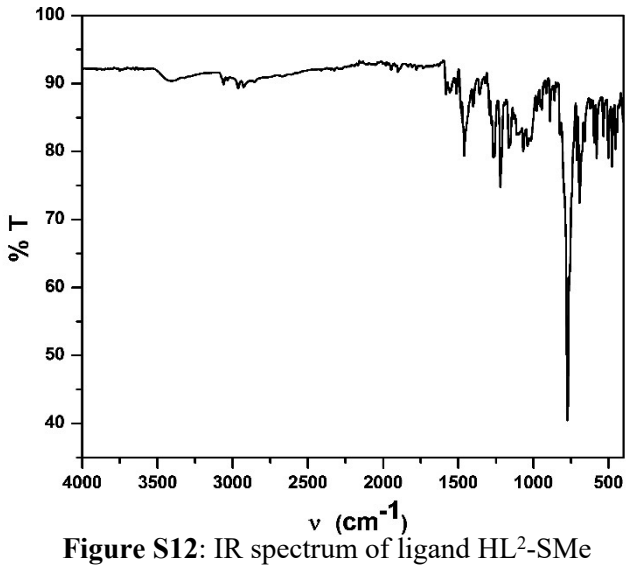

Figure S12: IR spectrum of ligand HL^2-SMe

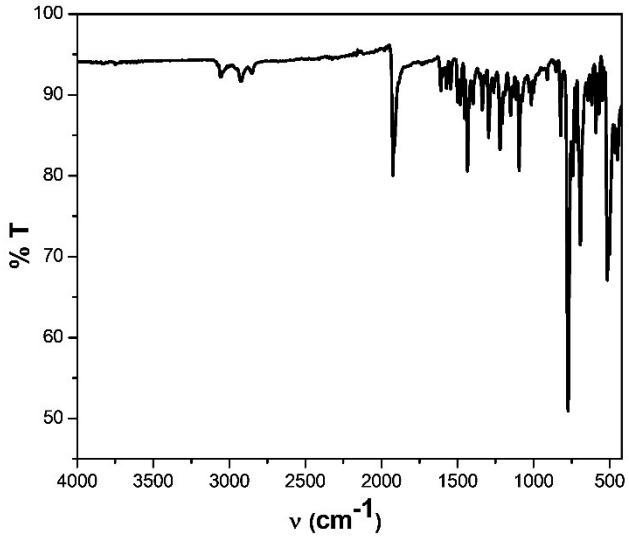

Figure S13: IR spectrum of complex **1**

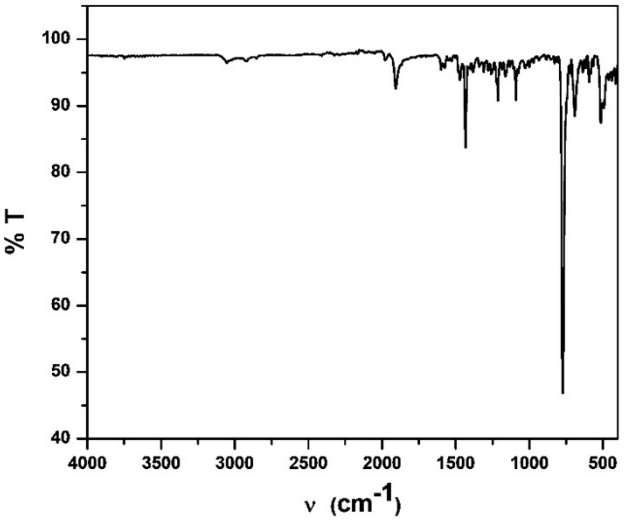

Figure S14: IR spectrum of complex **2**

Table S1. Crystallographic data and refinement parameters of complexes **1** and **2**

Complex	$[Ru(L^1)(CO)(PPh_3)_2]$ (**1**)	$[Ru(L^2)(CO)(PPh_3)_2]$ (**2**)
Formula	C53 H40 N2 O2 P2 Ru	C55 H42 N2 O2 P2 Ru
Formula Weight	899.88	925.91
Crystal System	*monoclinic*	*triclinic*
Space group	*C m*	*P -1*
a, b, c [Å]	18.2738(15), 15.3551(11), 9.8021(7)	10.5463(8), 12.0634(9), 17.8689(14)
α	90	76.220(2)
β	120.739(2)	86.297(2)
γ	90	86.034(2)
V [$Å^3$]	2364.0(3)	2199.9(3)
Z	2	2
D(calc) [g/cm^3]	1.264	1.398
Mu(MoKa) [/mm]	0.440	0.475
F(000)	924	952
Temperature (K)	293(2)	293(2)
Radiation [Å]	0.71073	0.71073
θ(Min-Max) [°]	2.417- 26.685	1.858- 26.420
Dataset (h; k; l)	-23 to 23, -19 to 19, -12 to 12	-13 to 13, -15 to 15, -22 to 22
R, wR_2	0.0343, 0.0643	0.0487, 0.1035
Goodness of fit(S)	1.066	1.149
CCDC No.	2262838	2262839

Table S2. Selected X-ray and calculated bond distances (Å) and angles (°) of complexes **1** and **2**

1			**2**		
Bonds(Å)	X-ray	Calc.	Bonds(Å)	X-ray	Calc.
Ru(1)- C(17)	1.853(7)	1.861	Ru(1)- C(2)	2.054(4)	2.058
Ru(1)- C(1)	2.046(6)	2.055	Ru(1)- C(1)	1.933(5)	1.866
Ru(1)- N(1)	2.069(6)	2.107	Ru(1)- N(1)	2.037(3)	2.085
Ru(1)- O(1)	2.192(4)	2.216	Ru(1)- O(2)	2.250(2)	2.238
Ru(1)- P(1)	2.3827(10)	2.438	Ru(1)- P(1)	2.3781(9)	2.439
N(1)-N(2)	1.274(7)	1.284	N(1)-N(2)	1.274(4)	1.277
O(2)-C(17)	1.151(8)	1.142	O(1)-C(1)	1.004(4)	1.114
Angles (°)					
C(17)-Ru(1)-C(1)	93.7(3)	97.970	C(1)-Ru(1)-C(2)	103.39(17)	98.747
C(17)-Ru(1)-N(1)	171.6(3)	175.729	C(1)-Ru(1)-N(1)	178.12(14)	175.736
C(1)-Ru(1)-N(1)	77.9(3)	77.759	C(2)-Ru(1)-N(1)	77.84(13)	76.989
C(17)-Ru(1)-O(1)	111.1(3)	108.598	C(1)-Ru(1)-O(2)	100.86(14)	107.993
C(1)-Ru(1)-O(1)	155.20(19)	153.431	C(2)-Ru(1)-O(2)	155.75(13)	153.257
N(1)-Ru(1)-O(1)	77.3(2)	75.671	N(1)-Ru(1)-O(2)	77.93(10)	76.270
C(17)-Ru(1)-P(1)	88.54(4)	88.296	C(1)-Ru(1)-P(1)	87.59(10)	88.536
C(1)-Ru(1)-P(1)	94.59(3)	92.849	C(2)-Ru(1)-P(1)	90.13(10)	92.780
N(1)-Ru(1)-P(1)	92.11(4)	91.896	N(1)-Ru(1)-P(1)	90.99(8)	91.567
O(1)-Ru(1)-P(1)	86.33(4)	88.041	O(2)-Ru(1)-P(1)	91.25(6)	88.248

Table S3. Energy and % of composition of some selected molecular orbitals of $[Ru(L^1)(CO)(PPh_3)_2]$ (**1**)

MO	Energy	% Composition			
		Ru	L^1	CO	PPh3
LUMO+5	-0.47	02	09	01	88
LUMO+4	-0.49	03	00	00	97
LUMO+3	-0.59	00	03	02	95
LUMO+2	-0.64	03	00	00	96
LUMO+1	-0.87	19	02	01	78
LUMO	-1.83	03	92	02	03
HOMO	-4.46	17	82	00	01
HOMO-1	-5.45	29	66	00	06
HOMO-2	-5.56	52	30	16	02
HOMO-3	-5.74	01	89	00	10
HOMO-4	-6.06	26	47	03	25
HOMO-5	-6.24	04	35	01	59
HOMO-6	-6.47	09	75	04	13
HOMO-7	-6.58	23	33	01	43
HOMO-8	-6.63	30	21	03	45
HOMO-9	-6.68	02	02	00	96
HOMO-10	-6.72	04	05	01	90

Table S4. Energy and % of composition of some selected molecular orbitals of $[Ru(L^2)(CO)(PPh_3)_2]$ (**2**)

MO	Energy	% Composition			
		Ru	L^2	CO	PPh3
LUMO+5	-0.50	03	03	01	93
LUMO+4	-0.52	02	00	00	97
LUMO+3	-0.63	00	02	02	97
LUMO+2	-0.68	03	00	00	96
LUMO+1	-0.92	19	02	01	77
LUMO	-1.92	04	90	03	03
HOMO	-4.51	15	83	00	02
HOMO-1	-5.48	28	66	00	06
HOMO-2	-5.61	51	31	15	02
HOMO-3	-5.84	09	86	01	04
HOMO-4	-6.13	15	24	00	61
HOMO-5	-6.44	16	40	03	42
HOMO-6	-6.48	00	99	00	01
HOMO-7	-6.61	30	50	05	16
HOMO-8	-6.68	06	26	01	67
HOMO-9	-6.70	09	18	00	72
HOMO-10	-6.72	01	11	01	87

Table S5: Vertical electronic transition calculated by TDDFT/CPCM method of complexes **1** and **2**

Compd.	λ (nm)	E (eV)	Osc. Strength (f)	Key excitations	Character	$\lambda_{expt.}$ (nm) (ε, $M^{-1}cm^{-1}$)
1	613.06	2.0224	0.1216	(94%)HOMO→LUMO	ILCT/MLCT	656 (5248)
	405.29	3.0592	0.1986	(92%)HOMO-1→LUMO	ILCT/MLCT	432 (8854)
	374.31	3.3123	0.1473	(93%)HOMO-3→LUMO	ILCT	364 (10196)
	332.91	3.7355	0.0633	(80%)HOMO-5→LUMO	ILCT	
2	637.97	1.9434	0.1192	(95%)HOMO→LUMO	ILCT/MLCT	682 (4419)
	427.45	2.9005	0.0524	(90%)HOMO-1→LUMO	ILCT/MLCT	434 (3828)
	370.20	3.3491	0.0543	(72%)HOMO-3→LUMO	ILCT	
	329.05	3.7680	0.1119	(70%)HOMO-6→LUMO	ILCT	319 (22914)

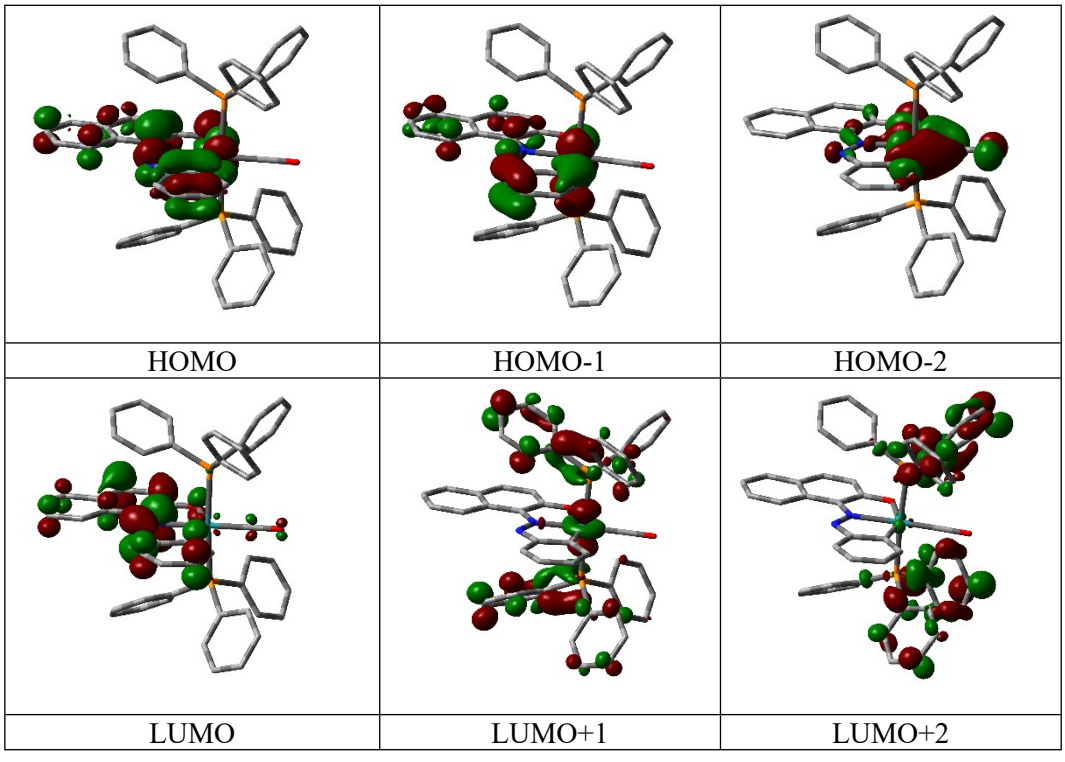

Figure S15. Contour plots of some selected molecular orbital of **1**

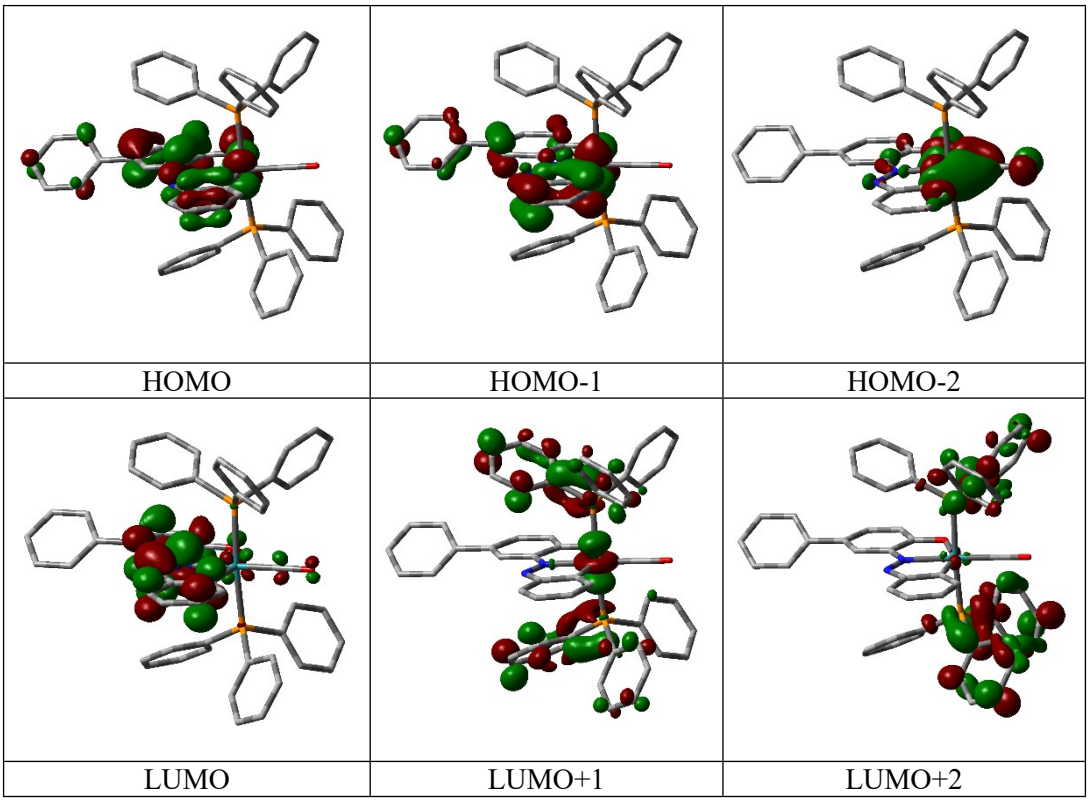

Figure S16. Contour plots of some selected molecular orbital of **2**

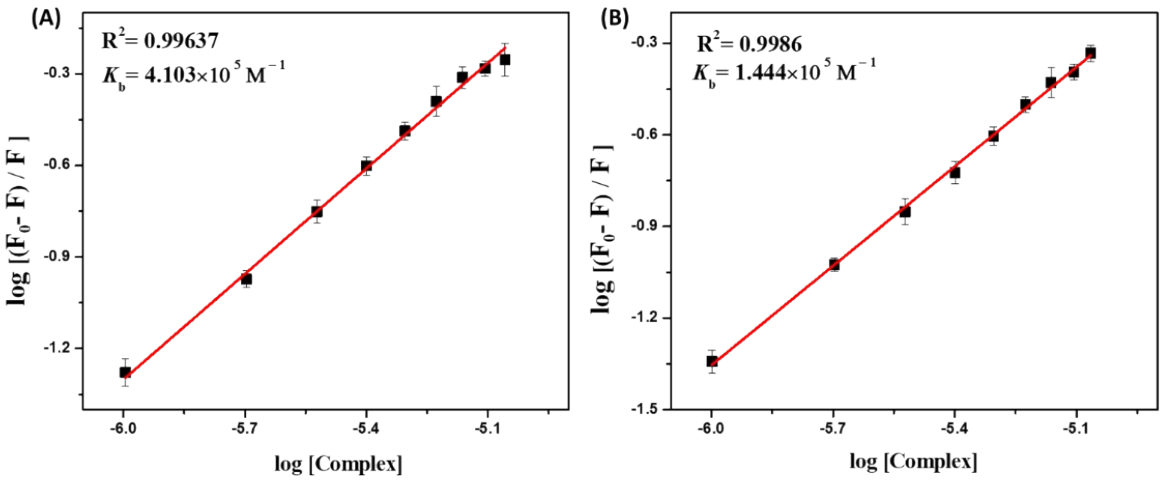

Figure S17. Plot of log [(F_o-F)/F] versus log [complex] of complexes **1** (A) and **2** (B)

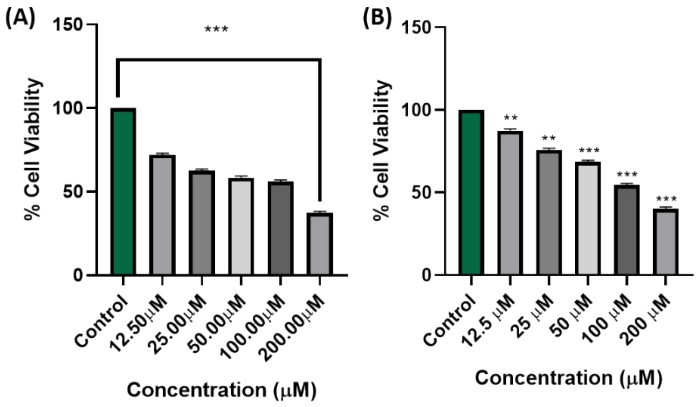

Figure S18. Percentage cell viability measured for HL^1-SEt (A) and HL^2-SMe (B) against MCF-7

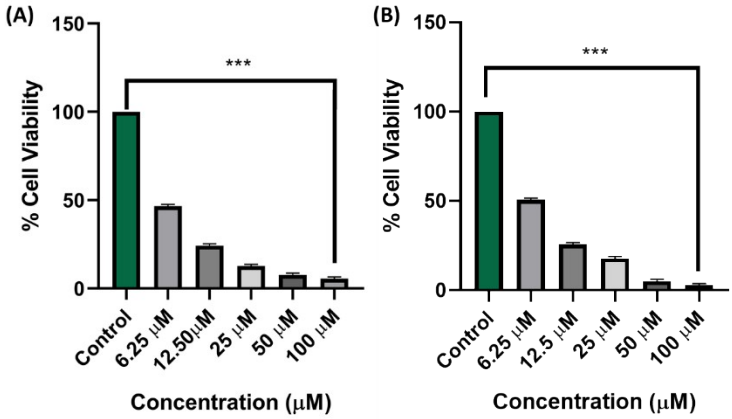

Figure S19. Percentage cell viability measured for complex **1** (A) and **2** (B) against MCF-7

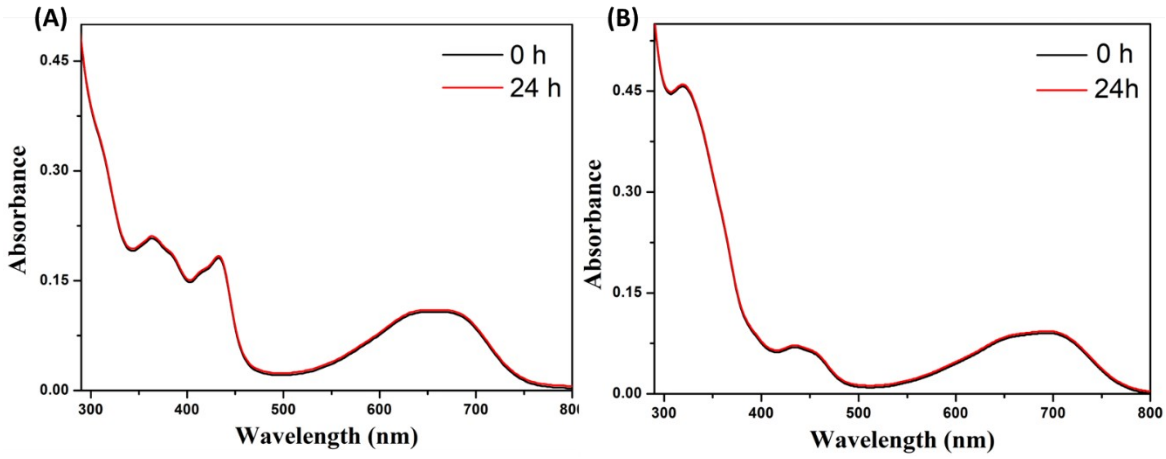

Figure S20. UV spectra of the metal complexes **1**(A) and **2**(B), showing their stability in 1:10 DMSO /buffer medium at 0 and 24 h.

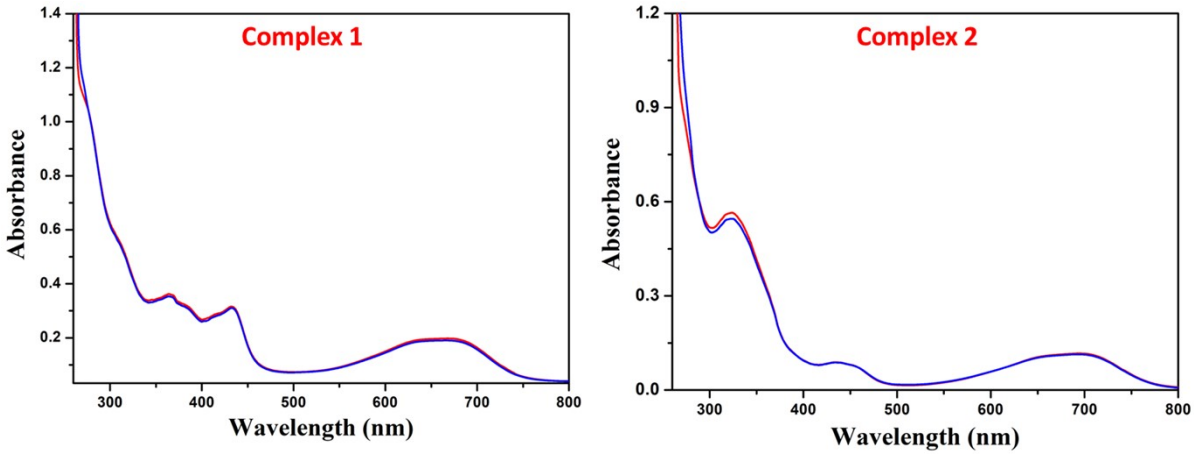

Figure S21: Absorption spectra of complexes (—) and after addition of BSA (—).